PNAS

Supporting Information for

Enhancing chimeric antigen receptor T cell therapy by modulating the p53 signaling network with Δ133p53α

Christopher Roselle[a,b], Izumi Horikawa[c], Linhui Chen[a], Andre S. Kelly[a], Donna Gonzales[a], Tong Da[a], Nils Wellhausen[a,b], Philipp C. Rommel[a,d], Daniel Baker[a,b,e], Megan Suhoski[a], John Scholler[a], Roddy S. O'Connor[a], Regina M. Young[a], Curtis C. Harris[c], and Carl H. June[a,d]

[a]Center for Cellular Immunotherapies, Perelman School of Medicine, University of Pennsylvania, Philadelphia, PA 19104, USA

[b]Perelman School of Medicine, University of Pennsylvania, Philadelphia, PA 19104, USA

[c] Laboratory of Human Carcinogenesis, Center for Cancer Research, National Cancer Institute, National Institutes of Health, Bethesda, MD 20892, USA

[d]Department of Pathology and Laboratory Medicine, Perelman School of Medicine, University of Pennsylvania, Philadelphia, PA 19104, USA

[e]Cardiovascular Institute, Department of Medicine, Perelman School of Medicine, University of Pennsylvania, PA 19104, USA

*Carl H. June

Email: cjune@upenn.edu

This PDF file includes:

Figures S1 to S9
Tables S1 to S2

Other supporting materials for this manuscript include the following:

N/A

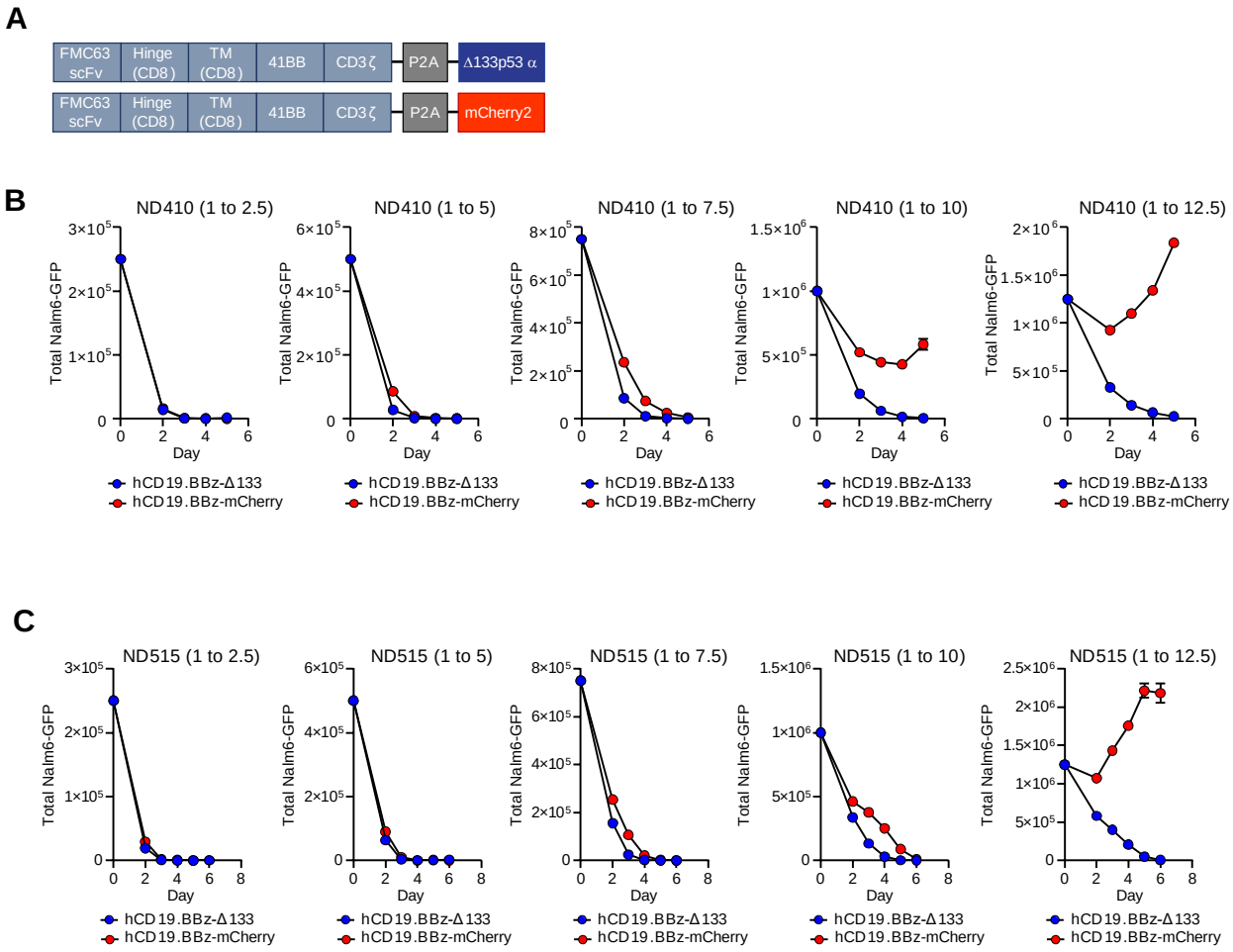

Fig. S1. Evaluation of Δ133-CARs expressing Δ133p53α downstream of P2A linker. (A) Construct maps of Δ133p53α- and mCherry2-expressing constructs with hCD19.BBz CAR upstream of P2A linker. (B) Tumor measurements over time from in vitro co-culture assay described in Figure 1D using CARs generated from healthy donor ND410. (C) Tumor measurements over time from in vitro co-culture assay described in Figure 1D using CARs generated from healthy donor ND410. Note that aside from the data presented in this figure, all other data in this manuscript was generated using CAR constructs with the CD19-directed CAR downstream of the P2A linker.

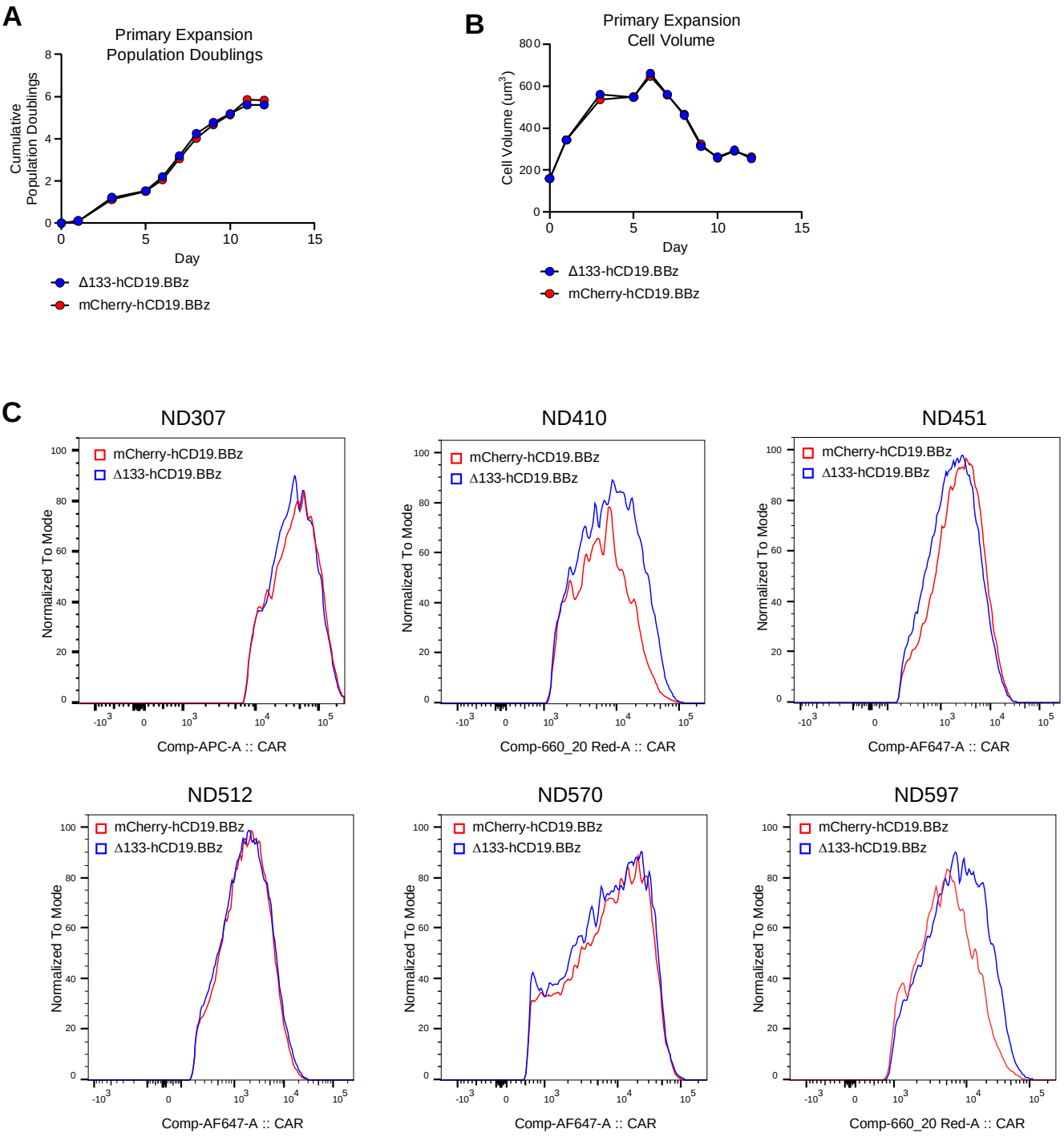

Fig. S2. Characterization of Δ133-CARs during primary expansion. (A) Representative proliferation curves of total T cells during primary expansion and (B) cell volume for Δ133- and WT CARs. No meaningful or consistent differences were observed during primary expansion with respect to proliferation or cell volume. (C) Surface CAR median fluorescence intensity (MFI) at the end of primary expansion for the six normal donors used in Figure 1E and 1F, as indicated by the header above each graph (i.e. “ND307”). Histograms shown were gated as follows: lymphocytes/single cells/live/CAR+.

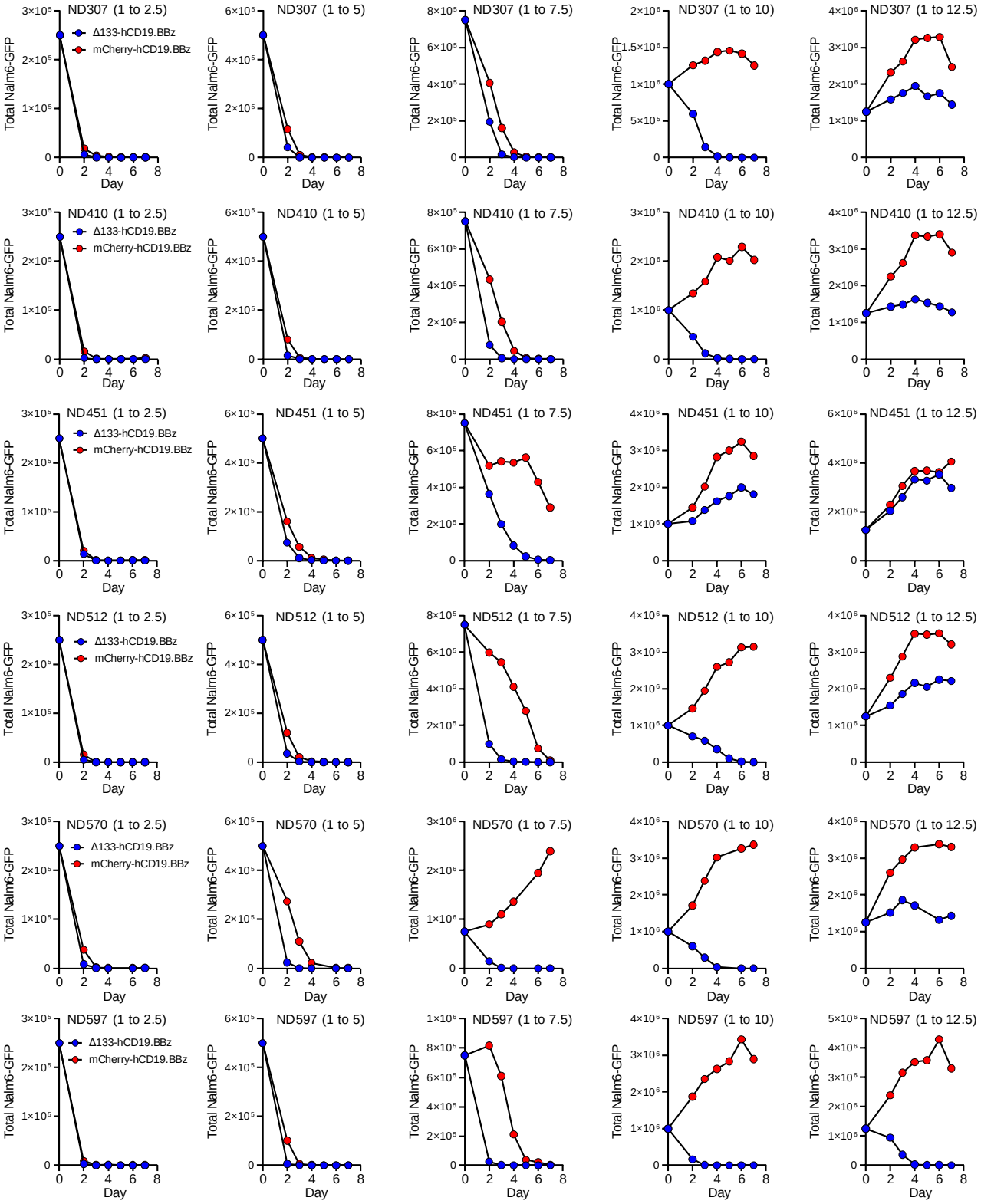

Fig. S3. Donor-specific tumor clearance curves for in vitro Nalm6 co-culture data shown in Figure 1E. Each row represents a different normal donor, indicated by the header above each graph. Each column represents a different E:T ratio, showing all five E:Ts that were evaluated: 1 to 2.5, 1 to 5, 1 to 7.5, 1 to 10, and 1 to 12.5. Each point represents the mean of two technical replicates. Error bars are not visible due to the size of each data point exceeding the range of the SEM.

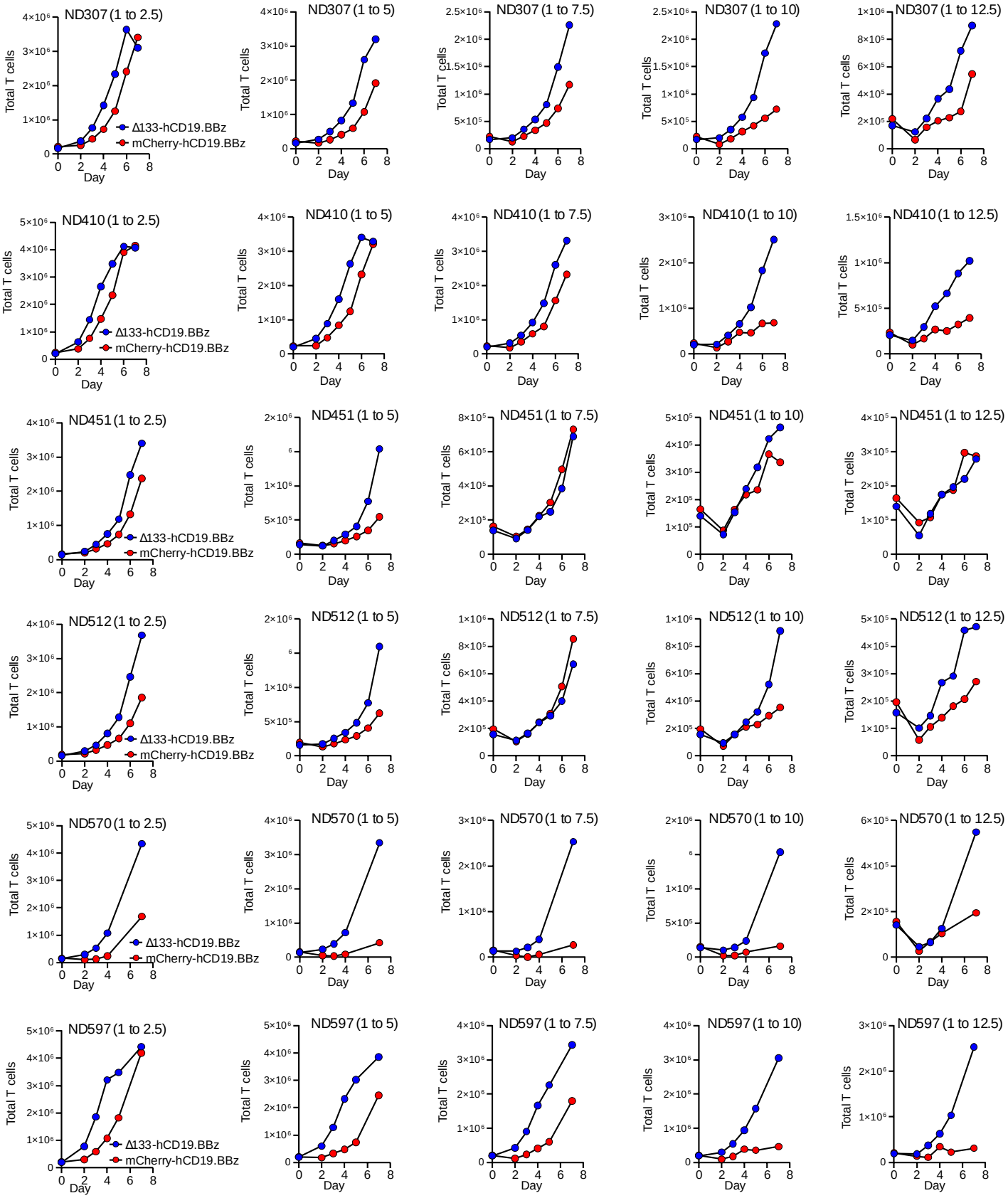

Fig. S4. Donor-specific proliferation curves from in vitro Nalm6 co-culture data shown in Figure 1F. Each row represents a different normal donor, indicated by the header above each graph. Each column represents a different E:T ratio, showing all five E:Ts that were evaluated: 1 to 2.5, 1 to 5, 1 to 7.5, 1 to 10, and 1 to 12.5. Each point represents the mean of two technical replicates. Error bars are not visible due to the size of each data point exceeding the range of the SEM.

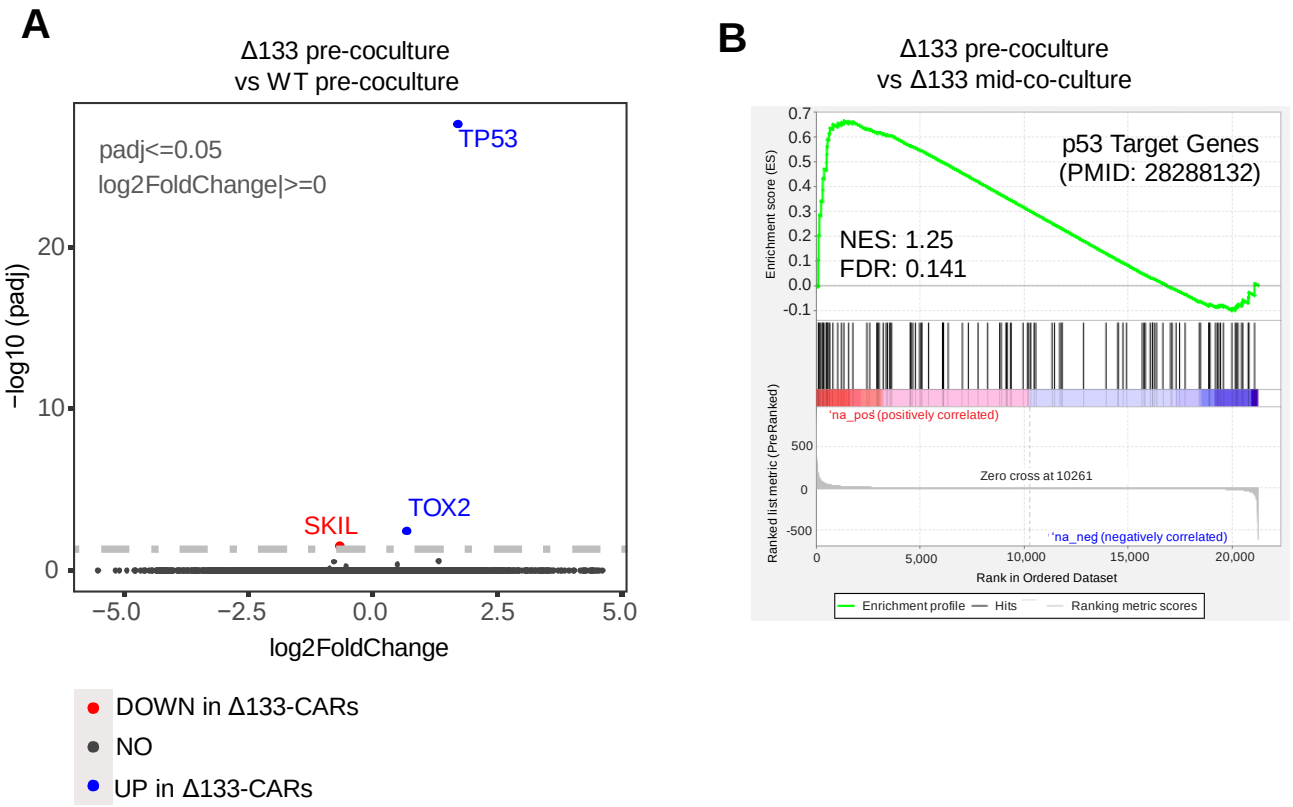

Fig. S5. RNAseq data for additional pairwise comparisons. (A) Volcano plot showing differentially expressed genes in WT and Δ133p53α-expressing CAR T cells isolated prior to co-culture. All genes with an adjusted p-value (padj) less than or equal to 0.05 are highlighted, with genes in red upregulated in the WT CARs (i.e. downregulated in Δ133-CARs) and gene in blue upregulated in Δ133-CARs. Note that TP53 is reflective of ectopic Δ133p53α expression. (B) Gene set enrichment analysis (GSEA) results for p53 Target Genes. Compared with Δ133-CARs pre-coculture, Δ133-CARs mid-coculture have an enrichment in expression of p53 target genes.

A ND307 hCD19.28z - 3x28 Bead Restimulation

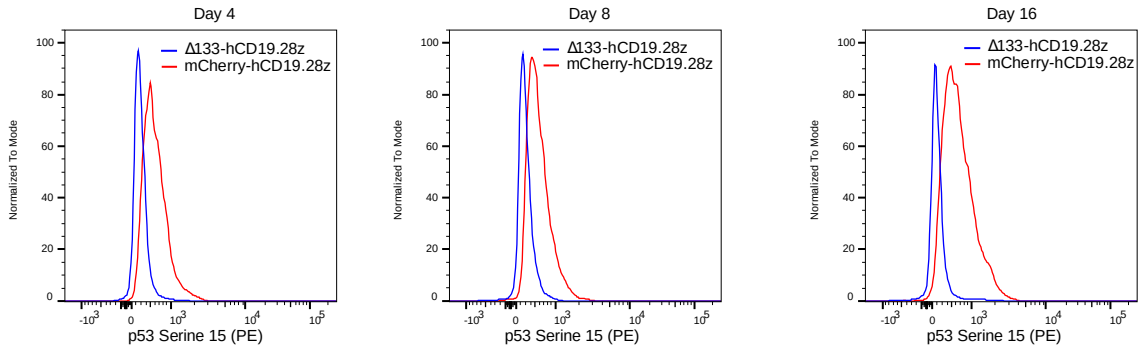

B ND569 hCD19.BBz - Nalm6 co-culture

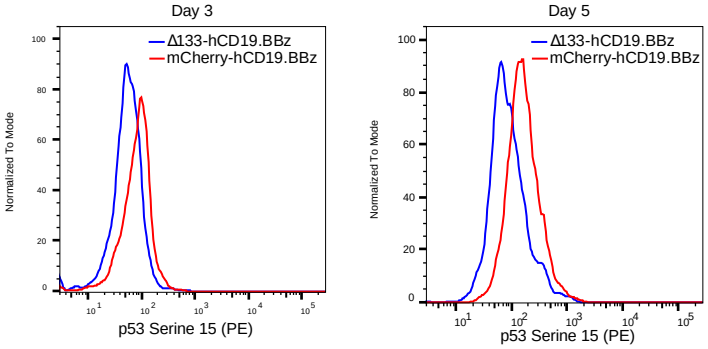

C ND569 hCD19.BBz - 3x28 Bead Restimulation

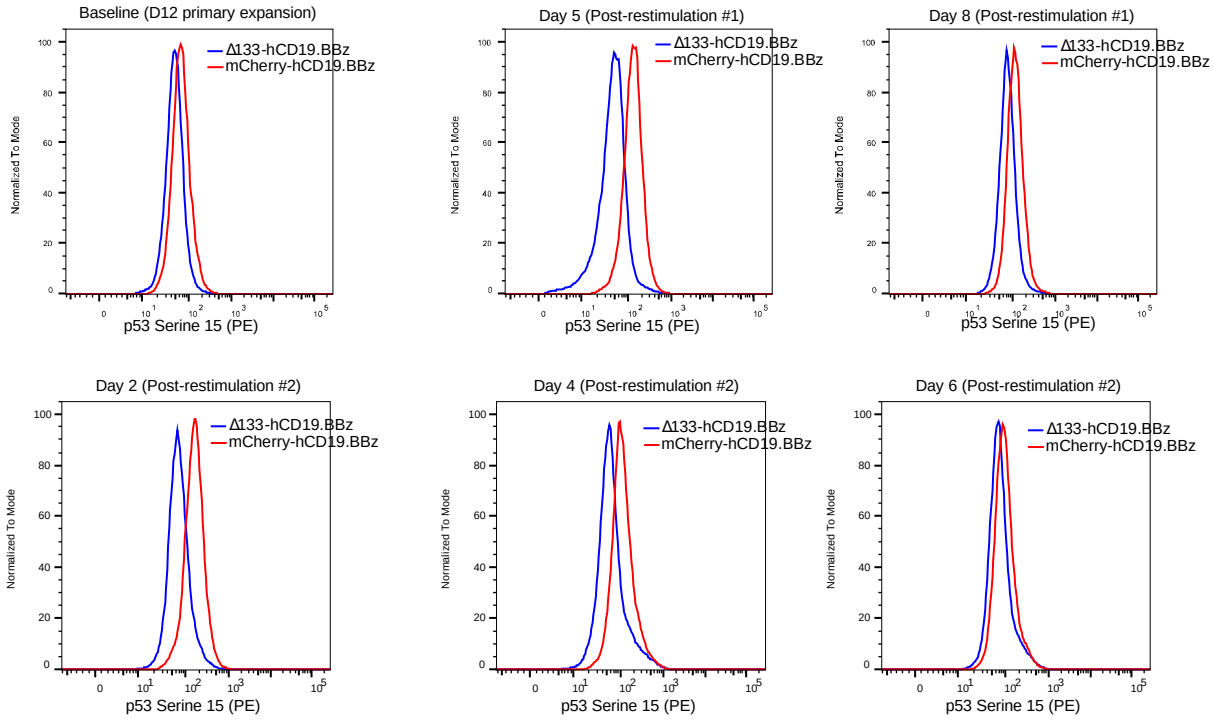

Fig. S6. Δ133-CARs have reduced phospho-p53 (serine 15) expression in multiple contexts. (A) Δ133-CARs with a CD28 costimulatory domain have markedly reduced expression of p53-S15 when restimulated post-expansion with magnetic beads coated with anti-CD3 and anti-CD28 antibodies. (B) Δ133-CARs with a 41BB costimulatory domain exhibit reduced p53-S15 expression when co-cultured with Nalm6-GFP leukemia cells and (C) when restimulated post-expansion with with magnetic beads coated with anti-CD3 and anti-CD28 antibodies. For each context in A-C, multiple time points are shown, as indicated by the header above each histogram.

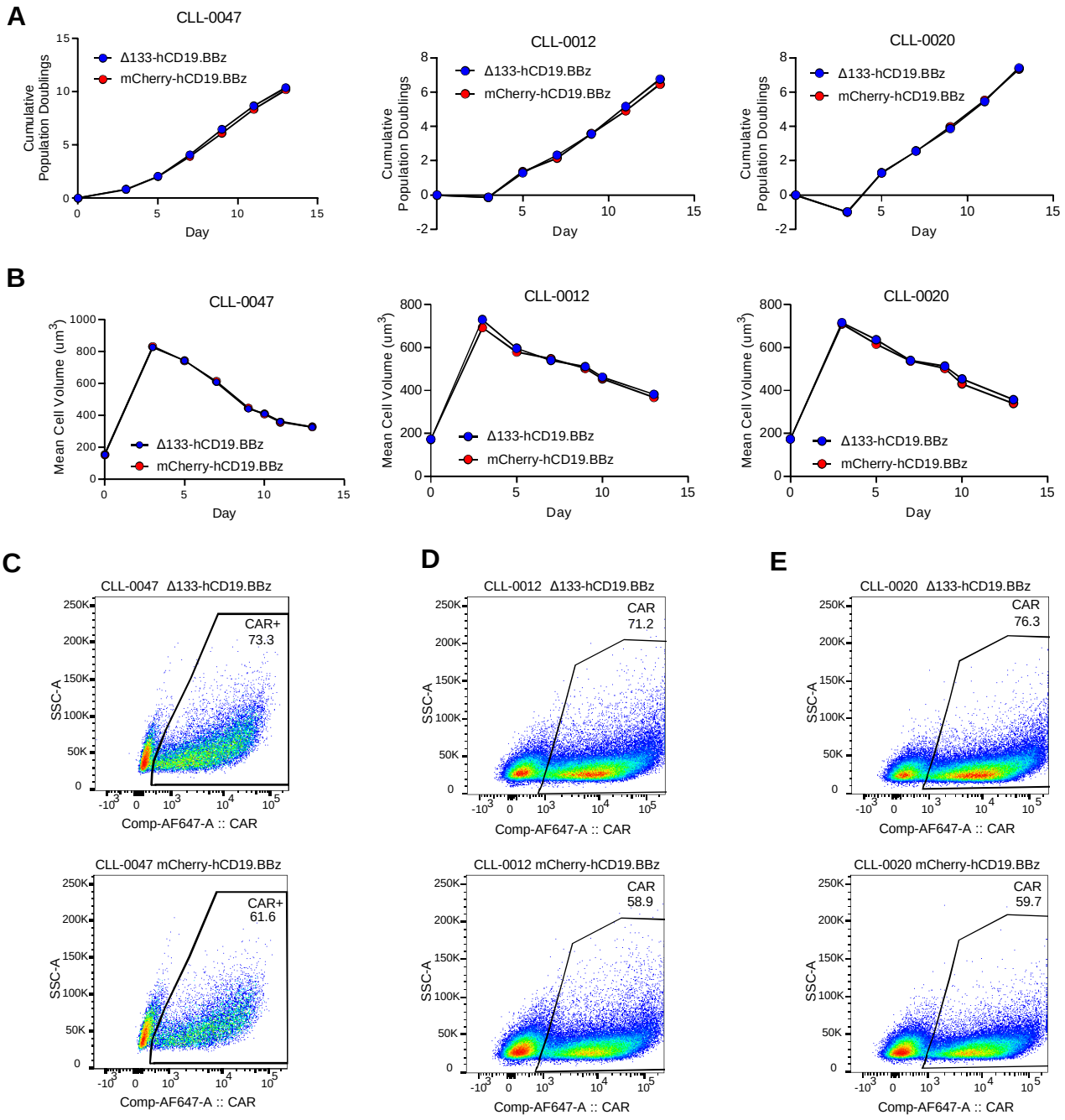

Fig. S7. Primary expansion characteristics of CLL-derived CAR T cells. (A) T cell proliferation during primary expansion for responding patient #0047 and non-responding patients #0012 and #0020. (B) Corresponding cell volumes during primary expansion at each time point for data shown in A. (C) Surface CAR expression demonstrates similar transduction efficiencies post-expansion for patient #0047. Δ133-CARs are shown in the top panel, with corresponding WT mCherry-expressing CARs in the bottom panel. The same is shown for patient #0012 in (D) and patient #0020 in (E).

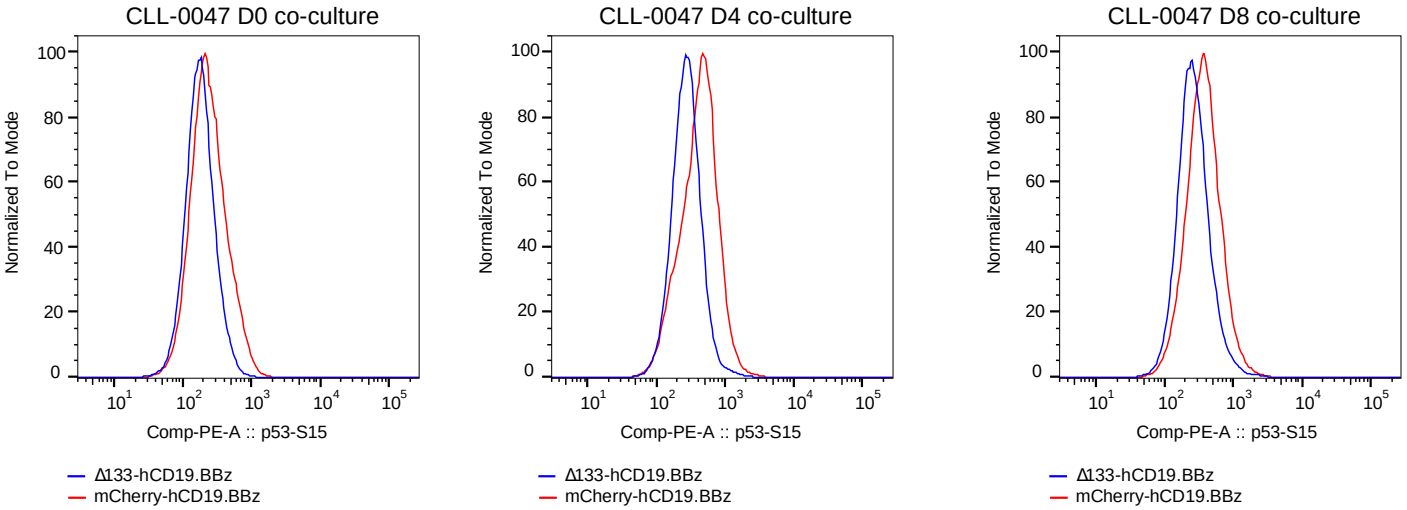

Fig. S8. Δ133-CARs generated from CLL patient #0047 have reduced p53-S15 expression during in vitro Nalm6-GFP co-culture.

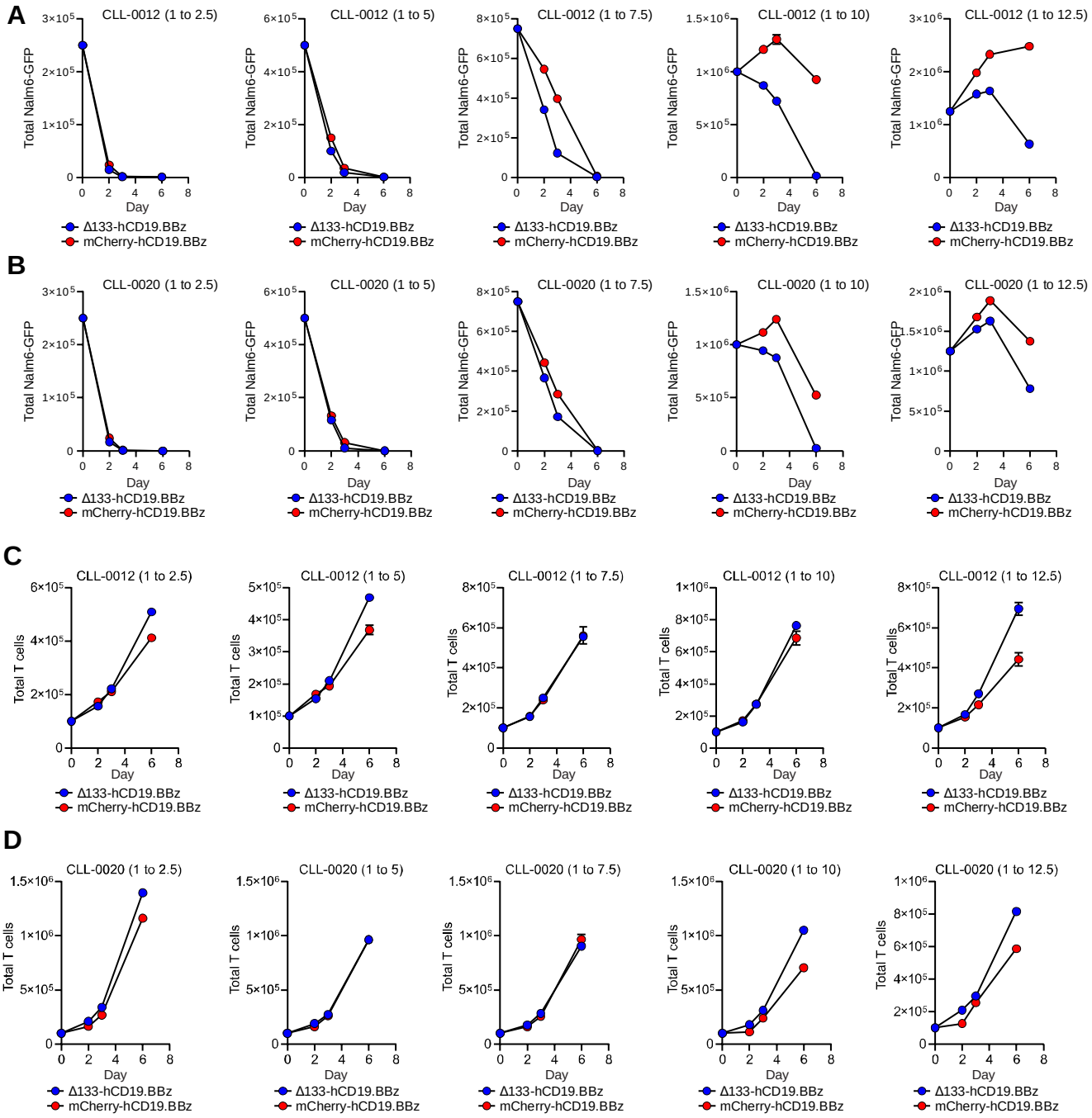

Fig. S9. Patient-specific tumor clearance and T cell proliferation curves during in vitro Nalm6-GFP co-culture. In (A) and (B) are the individual tumor clearance curves for the aggregated data shown in Figure 4C for patients #0012 and #0020, respectively, as indicated by the header above each graph. In (C) and (D) are the corresponding T cell proliferation curves for patients #0012 and #0020, respectively, again indicated by the header above each graph.

Table S1. Top 100 differentially expressed genes with p-adjusted ≤ 0.05 sorted by the magnitude of log2 fold change.

Rank	ID	Gene.name	Up/Down	log2FoldChange	padj
1	ENSG00000168453	HR	DOWN	-3.65	1.69E-10
2	ENSG00000204866	IGFL2	DOWN	-3.62	9.81E-04
3	ENSG00000222012	AC005481.1	DOWN	-3.37	2.48E-03
4	ENSG00000280969	RPS4Y2	DOWN	-3.22	2.46E-03
5	ENSG00000260386	LINC01225	DOWN	-3.11	2.23E-04
6	ENSG00000204960	BLACE	DOWN	-2.78	8.54E-04
7	ENSG00000099864	PALM	DOWN	-2.56	3.17E-15
8	ENSG00000015413	DPEP1	DOWN	-2.56	1.69E-10
9	ENSG00000229417	NPM1P25	DOWN	-2.54	1.04E-02
10	ENSG00000099866	MADCAM1	DOWN	-2.46	1.04E-02
11	ENSG00000127324	TSPAN8	DOWN	-2.45	1.73E-05
12	ENSG00000245213	AC105285.1	DOWN	-2.44	3.44E-03
13	ENSG00000145194	VWA5B2	DOWN	-2.33	1.79E-02
14	ENSG00000069812	HES2	DOWN	-2.28	9.10E-03
15	ENSG00000257108	NHLRC4	DOWN	-2.25	3.74E-02
16	ENSG00000173227	SYT12	DOWN	-2.23	2.52E-04
17	ENSG00000183638	RP1L1	DOWN	-2.23	2.23E-04
18	ENSG00000101332	CCM2L	DOWN	-2.23	4.63E-02
19	ENSG00000101194	NKAIN4	DOWN	-2.21	2.15E-09
20	ENSG00000151892	GFRA1	DOWN	-2.18	1.38E-06
21	ENSG00000169242	EFNA1	DOWN	-2.17	8.55E-03
22	ENSG00000235621	LINC00494	DOWN	-2.15	4.81E-02
23	ENSG00000279024	AC112255.1	DOWN	-2.12	2.79E-02
24	ENSG00000105472	CLEC11A	DOWN	-2.10	9.19E-11
25	ENSG00000176884	GRIN1	DOWN	-2.08	6.25E-04
26	ENSG00000185738	NRG3	DOWN	-2.08	3.80E-03
27	ENSG00000185028	LRRC14B	DOWN	-2.08	4.87E-07
28	ENSG00000214357	NEURL1B	DOWN	-2.07	2.44E-09
29	ENSG00000092377	TBL1Y	DOWN	-2.05	1.33E-05
30	ENSG00000226859	LINC02051	DOWN	-2.04	2.39E-03
31	ENSG00000170834	CEL	DOWN	-2.03	2.87E-03
32	ENSG00000176434	CLEC14A	DOWN	-2.00	1.61E-07
33	ENSG00000235888	AF064858.1	DOWN	-1.98	4.62E-05
34	ENSG00000261159	AC112484.3	DOWN	-1.97	3.13E-08
35	ENSG00000254319	AC246817.2	DOWN	-1.95	1.20E-03
36	ENSG00000231419	LINC00689	DOWN	-1.93	2.77E-03
37	ENSG00000162591	MEGF6	DOWN	-1.93	9.60E-03
38	ENSG00000263667	AL035696.3	DOWN	-1.88	9.37E-04
39	ENSG00000108551	RASD1	DOWN	-1.88	6.36E-06
40	ENSG00000164362	TERT	DOWN	-1.87	1.02E-04
41	ENSG00000172201	ID4	DOWN	-1.86	4.11E-07
42	ENSG00000040608	RTN4R	DOWN	-1.84	1.46E-04
43	ENSG00000224016	AC092681.1	DOWN	-1.83	3.15E-02
44	ENSG00000198429	ZNF69	DOWN	-1.82	2.99E-02
45	ENSG00000205978	NYNRIN	DOWN	-1.80	3.37E-06
46	ENSG00000100027	YPEL1	DOWN	-1.79	2.46E-04
47	ENSG00000257275	AL139020.1	DOWN	-1.79	2.13E-03
48	ENSG00000165810	BTNL9	DOWN	-1.79	2.69E-02
49	ENSG00000130635	COL5A1	DOWN	-1.78	2.65E-18
50	ENSG00000180869	LINC01559	DOWN	-1.76	1.04E-03
51	ENSG00000130202	NECTIN2	DOWN	-1.75	7.31E-03
52	ENSG00000004809	SLC22A16	DOWN	-1.75	3.03E-02
53	ENSG00000102935	ZNF423	DOWN	-1.75	2.46E-02
54	ENSG00000224940	PRRT4	DOWN	-1.74	2.50E-03
55	ENSG00000167693	NXN	DOWN	-1.73	1.61E-07
56	ENSG00000267060	PTGES3L	DOWN	-1.73	3.65E-04
57	ENSG00000261434	AC021087.4	DOWN	-1.73	7.70E-03
58	ENSG00000166897	ELFN2	DOWN	-1.72	6.71E-09
59	ENSG00000176533	GNG7	DOWN	-1.72	9.78E-12
60	ENSG00000175287	PHYHD1	DOWN	-1.70	8.05E-06
61	ENSG00000002745	WNT16	DOWN	-1.67	2.28E-03
62	ENSG00000182175	RGMA	DOWN	-1.67	2.07E-02
63	ENSG00000272733	AP000345.2	DOWN	-1.67	4.07E-06
64	ENSG00000095932	SMIM24	DOWN	-1.66	4.59E-06
65	ENSG00000065717	TLE2	DOWN	-1.65	7.92E-04
66	ENSG00000035862	TIMP2	DOWN	-1.65	1.01E-15
67	ENSG00000172995	ARPP21	DOWN	-1.64	5.80E-10
68	ENSG00000225978	HAR1A	DOWN	-1.63	4.78E-04
69	ENSG00000112559	MDFI	DOWN	-1.63	7.70E-09
70	ENSG00000267924	AC139769.2	DOWN	-1.62	6.36E-06
71	ENSG00000267731	AC005332.3	DOWN	-1.61	2.60E-04
72	ENSG00000184702	SEPTIN5	DOWN	-1.61	1.82E-04
73	ENSG00000006534	ALDH3B1	DOWN	-1.61	4.25E-03
74	ENSG00000135116	HRK	DOWN	-1.61	2.50E-03
75	ENSG00000174807	CD248	DOWN	-1.60	8.42E-06
76	ENSG00000187621	TCL6	DOWN	-1.60	4.25E-03
77	**ENSG00000177694**	**NAALADL2**	**UP**	**1.59**	**2.71E-02**
78	ENSG00000168916	ZNF608	DOWN	-1.59	8.74E-11
79	ENSG00000167996	VWCE	DOWN	-1.57	1.74E-04
80	ENSG00000176678	FOXL1	DOWN	-1.57	2.83E-07
81	ENSG00000067606	PRKCZ	DOWN	-1.57	8.73E-05
82	ENSG00000196781	TLE1	DOWN	-1.56	2.67E-03
83	ENSG00000189337	KAZN	DOWN	-1.56	1.60E-05
84	ENSG00000225138	SLC9A3-AS1	DOWN	-1.56	3.35E-02
85	ENSG00000162736	VANGL2	DOWN	-1.55	9.08E-04
86	ENSG00000100968	NFATC4	DOWN	-1.55	4.28E-06
87	ENSG00000171056	SOX7	DOWN	-1.54	1.37E-05
88	ENSG00000180773	ANKRD30B	DOWN	-1.54	6.25E-04
89	ENSG00000160678	S100A1	DOWN	-1.54	1.63E-02
90	ENSG00000099889	ARVCF	DOWN	-1.53	2.23E-03
91	ENSG00000087076	HSD17B14	DOWN	-1.53	6.40E-03
92	ENSG00000241956	AC109466.1	DOWN	-1.52	3.13E-05
93	ENSG00000211978	IGHV5-78	DOWN	-1.52	4.89E-07
94	ENSG00000227051	C14orf132	DOWN	-1.52	2.08E-06
95	ENSG00000004399	PLXND1	DOWN	-1.51	1.69E-10
96	ENSG00000108405	P2RX1	DOWN	-1.51	1.83E-03
97	ENSG00000157985	AGAP1	DOWN	-1.51	1.00E-06
98	ENSG00000131653	KREMEN2	DOWN	-1.51	1.68E-03
99	ENSG00000238121	LINC00426	DOWN	-1.50	3.49E-05
100	ENSG00000169574	VPREB1	DOWN	-1.49	1.49E-05

Table S2. Gene sets enriched in Δ133-CARs and WT CARs with False discovery rate (FDR) < 0.1

Gene Set	NES	NOM p-val	FDR q-val
GOBP_RIBOSOME_BIOGENESIS	2.08	0	0
HALLMARK_MYC_TARGETS_V2	2.07	0	0
GOBP_RNA_MODIFICATION	2.01	0	0
GOBP_RRNA_PROCESSING	1.99	0	0
HALLMARK_MYC_TARGETS_V1	1.99	0	0
GOBP_CELLULAR_RESPONSE_TO_HEAT	1.95	0	0
GOBP_REGULATION_OF_TELOMERE_MAINTENANCE	1.93	0	0
GOBP_RNA_SPLICING_VIA_TRANSESTERIFICATION_REACTIONS	1.91	0	0
GOBP_POSITIVE_REGULATION_OF_TELOMERE_MAINTENANCE	1.88	0	0.001
GOBP_TRNA_MODIFICATION	1.87	0	0.001
GOBP_POSITIVE_REGULATION_OF_TRANSCRIPTION_BY_RNA_POLYMERASE_I	1.86	0	0.001
GOBP_MITOCHONDRIAL_GENE_EXPRESSION	1.86	0	0.001
GOBP_TRNA_PROCESSING	1.85	0	0.001
GOBP_RNA_METHYLATION	1.85	0	0.001
GOBP_RRNA_METABOLIC_PROCESS	1.83	0	0.002
GOBP_MITOCHONDRIAL_TRANSLATION	1.82	0	0.003
GOBP_REGULATION_OF_MRNA_PROCESSING	1.81	0	0.003
GOBP_POSITIVE_REGULATION_OF_CHROMOSOME_ORGANIZATION	1.81	0	0.003
GOBP_POSITIVE_REGULATION_OF_DNA_BIOSYNTHETIC_PROCESS	1.8	0	0.004
GOBP_TRANSCRIPTION_BY_RNA_POLYMERASE_III	1.79	0	0.004
GOBP_REGULATION_OF_TRANSCRIPTION_BY_RNA_POLYMERASE_III	1.78	0	0.005
GOBP_MITOCHONDRIAL_RNA_METABOLIC_PROCESS	1.75	0	0.011
GOBP_REGULATION_OF_HETEROTYPIC_CELL_CELL_ADHESION	1.74	0	0.016
GOBP_REGULATION_OF_TRANSLATIONAL_INITIATION	1.74	0.005	0.015
GOBP_MATURATION_OF_5_8S_RRNA	1.74	0.007	0.015
GOBP_REGULATION_OF_RNA_SPLICING	1.73	0	0.016
GOBP_RRNA_MODIFICATION	1.73	0	0.015
GOBP_TRANSLATIONAL_INITIATION	1.73	0	0.015
GOBP_REGULATION_OF_TELOMERE_MAINTENANCE_VIA_TELOMERE_LENGTHENING	1.73	0.003	0.016
GOBP_TYROSINE_PHOSPHORYLATION_OF_STAT_PROTEIN	1.72	0	0.017
GOBP_LYMPHOCYTE_CHEMOTAXIS	1.72	0	0.016
GOBP_MATURATION_OF_SSU_RRNA	1.72	0.002	0.017
GOBP_TRNA_METHYLATION	1.71	0.002	0.021
GOBP_REGULATION_OF_MRNA_SPLICING_VIA_SPLICEOSOME	1.71	0	0.021
GOBP_POSITIVE_REGULATION_OF_TELOMERE_MAINTENANCE_VIA_TELOMERE_LENGTHENING	1.71	0.004	0.021
GOBP_SPLICEOSOMAL_COMPLEX_ASSEMBLY	1.71	0	0.021
GOBP_ALTERNATIVE_MRNA_SPLICING_VIA_SPLICEOSOME	1.7	0.006	0.023
GOBP_RNA_5_END_PROCESSING	1.7	0.001	0.023
GOBP_T_HELPER_17_CELL_DIFFERENTIATION	1.68	0.004	0.031
GOBP_POSITIVE_REGULATION_OF_MRNA_METABOLIC_PROCESS	1.68	0	0.033
GOBP_NEGATIVE_REGULATION_OF_ADAPTIVE_IMMUNE_RESPONSE	1.67	0.002	0.041
GOBP_DNA_TEMPLATED_DNA_REPLICATION	1.67	0	0.041
GOBP_MRNA_MODIFICATION	1.66	0.005	0.042
GOBP_POSITIVE_REGULATION_OF_TRANSCRIPTION_BY_RNA_POLYMERASE_III	1.66	0.002	0.041
GOBP_POSITIVE_REGULATION_OF_RNA_SPLICING	1.66	0.007	0.042
GOBP_CD4_POSITIVE_OR_CD8_POSITIVE_ALPHA_BETA_T_CELL_LINEAGE_COMMITMENT	1.66	0.002	0.045
GOBP_NEGATIVE_REGULATION_OF_SIGNALING_RECEPTOR_ACTIVITY	1.64	0.004	0.057
GOBP_MATURATION_OF_SSU_RRNA_FROM_TRICISTRONIC_RRNA_TRANSCRIPT_SSU_RRNA_5_8S_RRNA_LSU_RRNA	1.64	0.002	0.057
GOBP_RRNA_METHYLATION	1.64	0.004	0.059
GOBP_POSITIVE_REGULATION_OF_TELOMERASE_ACTIVITY	1.64	0.005	0.059
GOBP_RNA_CAPPING	1.63	0.006	0.06
GOBP_CLEAVAGE_INVOLVED_IN_RRNA_PROCESSING	1.63	0.005	0.061
GOBP_TELOMERASE_RNA_LOCALIZATION	1.63	0.008	0.061
GOBP_POSITIVE_REGULATION_OF_TYROSINE_PHOSPHORYLATION_OF_STAT_PROTEIN	1.63	0.005	0.063
GOBP_REGULATION_OF_RRNA_PROCESSING	1.62	0.004	0.066
GOBP_TRANSCRIPTION_BY_RNA_POLYMERASE_I	1.62	0.014	0.071
GOBP_MATURATION_OF_LSU_RRNA	1.62	0.005	0.07
GOBP_CHRONIC_INFLAMMATORY_RESPONSE	1.62	0.001	0.069
GOBP_NEGATIVE_REGULATION_OF_CYTOKINE_PRODUCTION_INVOLVED_IN_IMMUNE_RESPONSE	1.62	0.014	0.068
GOBP_TELOMERE_MAINTENANCE_IN_RESPONSE_TO_DNA_DAMAGE	1.62	0.013	0.067
GOBP_TRANSLATIONAL_TERMINATION	1.62	0.004	0.066
GOBP_MATURATION_OF_5_8S_RRNA_FROM_TRICISTRONIC_RRNA_TRANSCRIPT_SSU_RRNA_5_8S_RRNA_LSU_RRNA	1.61	0.011	0.071
GOBP_REGULATION_OF_HUMORAL_IMMUNE_RESPONSE	1.61	0.01	0.075
GOBP_RESPONSE_TO_NICOTINE	1.6	0.015	0.077
GOBP_GPI_ANCHOR_METABOLIC_PROCESS	1.6	0.011	0.078
GOBP_POSITIVE_REGULATION_OF_TRANSLATIONAL_INITIATION	1.6	0.007	0.078
GOBP_RNA_PHOSPHODIESTER_BOND_HYDROLYSIS_EXONUCLEOLYTIC	1.6	0.015	0.077
GOBP_IRON_SULFUR_CLUSTER_ASSEMBLY	1.59	0.009	0.084
GOBP_ISOTYPE_SWITCHING_TO_IGG_ISOTYPES	1.59	0.006	0.093
GOBP_NEGATIVE_REGULATION_OF_CD4_POSITIVE_ALPHA_BETA_T_CELL_ACTIVATION	1.59	0.011	0.092
GOBP_T_HELPER_CELL_LINEAGE_COMMITMENT	1.59	0.006	0.092
GOBP_MONOUBIQUITINATED_PROTEIN_DEUBIQUITINATION	1.58	0.017	0.091
GOBP_MITOCHONDRIAL_RNA_PROCESSING	1.58	0.015	0.093
GOBP_DNA_TEMPLATED_DNA_REPLICATION_MAINTENANCE_OF_FIDELITY	1.58	0.011	0.093
GOBP_REGULATION_OF_TELOMERE_MAINTENANCE_IN_RESPONSE_TO_DNA_DAMAGE	1.58	0.013	0.093
GOBP_RNA_3_END_PROCESSING	1.58	0	0.092
GOBP_REGULATION_OF_T_HELPER_17_TYPE_IMMUNE_RESPONSE	1.58	0.012	0.095
GOBP_REGULATION_OF_MITOCHONDRIAL_GENE_EXPRESSION	1.58	0.019	0.094
GOBP_ENDONUCLEOLYTIC_CLEAVAGE_INVOLVED_IN_RRNA_PROCESSING	1.58	0.011	0.095
GOBP_REGULATION_OF_MITOCHONDRIAL_TRANSLATION	1.57	0.013	0.097
GOBP_ENDODERMAL_CELL_DIFFERENTIATION	-1.44	0	0.091